

# A Monolayer Complex of $\text{Cu}_2(\text{OH})_3\text{C}_{12}\text{H}_{25}\text{SO}_4$ Directly Precipitated from an Aqueous SDS Solution

Masaharu Okazaki,\* Kazumi Toriyama, Shinji Tomura, Taiji Kodama, and Eiji Watanabe

National Industrial Research Institute of Nagoya, Hirate, Kita-ku, Nagoya, 462-8510, Japan

Received January 27, 2000

A layered complex with the chemical composition of  $\text{Cu}_2(\text{OH})_3\text{C}_{12}\text{H}_{25}\text{OSO}_3$  was obtained through direct precipitation from a sodium dodecyl sulfate micellar solution of Cu(II) at a nearly neutral condition ( $\text{pH} \approx 6.8$ ). From the XRD,  $^{13}\text{C}$  CP/MAS NMR, and the spin probe ESR observations, a modified botallackite structure with a monolayer alkyl phase was proposed for the complex. Magnetic susceptibility measurements for the complex showed that there exist at least two exchange couplings: one is positive, and its magnitude is larger than that of the other, which is negative ( $J \approx -8$  K). Although the cupric ions of the complex are paramagnetic, most of those are ESR silent and only the ESR signals from defects could be observed even at 298 K. A spin clustering model has been employed to explain the magnetic properties of the complex.

## Introduction

Many basic cupric salts with lamellar structure having an alkyl layer between the two Cu(II) layers were synthesized, and their magnetic properties have been studied.<sup>1–4</sup> For example, a series of  $\text{Cu}_2(\text{OH})_3\text{RCOO}$  ( $\text{R} = \text{C}_n\text{H}_{2n+1}$ ) were obtained by replacing the acetate group of  $\text{Cu}(\text{OH})_3\text{CH}_3\text{COO}$  with  $\text{RCOO}^-$ . The structure and the characteristic magnetism of these materials are a recent matter of concern.<sup>2,3</sup> This is because a new type of molecular arrangement and interaction between the inorganic metal ion layer and the organic layer would offer a new function and/or a novel chemical property for, e.g., an efficient catalyst. In general a basic cupric salt, such as cupric hydroxy halides  $\text{Cu}_2(\text{OH})_3\text{X}$ , exhibits one of the three main crystal structures: botallackite, paratacamite, and atacamite.<sup>5,6</sup> The latter two are the three-dimensional ones and thus cannot form a layered structure. On the other hand, botallackite has a two-dimensional layered structure and thus is suitable to accommodate an alkyl layer between the two cupric hydroxide layers. The layered compounds are also classified by the structure of the alkyl layer: one is bilayer, and the other is monolayer. The chemical and physical characters of the complex are profoundly dependent on which type of structure is adopted. For example, only the bilayered structure is observed in the biological systems as the cell membrane.<sup>7</sup> Fujita et al. asserted that basic cupric salts with a carboxylate anion having a long alkyl chain adopt a bilayered structure of the botallackite type.<sup>2,3</sup> According to this structure [ $b = 0.613$  nm,  $c = 0.563$  nm,  $n_{\text{RCOOH}}$  (number of alkylcarboxylates in unit cell) = 2],<sup>6</sup> however, the two nearest alkyl chains extruded to the same interlayer space from the same

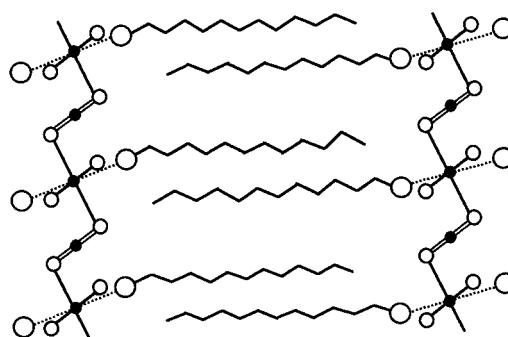


**Figure 1.** Schematic model (*ac* plane) for a basic copper salt with an anion having a long alkyl group. This structure is a modification of the botallackite ( $\text{Cu}_2(\text{OH})_3\text{Cl}$ ) type, where the Cl ion is replaced with, e.g., an alkyl sulfate anion. Thus, the large circle indicates the  $\text{SO}_4^-$  group of the alkyl sulfate anion. Small open and closed circles indicate the OH anion and the cupric ion, respectively. Duplex lines indicate the projection of the  $\text{Cu}(\text{OH})_2$  polymer-like chain. This is the model structure for the complex synthesized in the present study.

Cu(II) layer are far separated, ca. 0.56 nm, and it appears difficult for the alkyl chains to fill the space.

In the present study, we prepared a novel basic cupric (II) salt with dodecyl sulfate (DS) anion. We employed the direct precipitation method to prepare the complex in a way similar to that employed in the “template synthesis” of a nanostructured material.<sup>8,9</sup> The complex was characterized by means of XRD (X-ray diffraction), ESR, CP/MAS NMR, magnetic susceptibility measurement, and chemical analyses. From these observations we concluded that the system has a monolayered structure of the botallackite type, which is shown as Figure 1. In addition, an interesting observation is that most of the cupric ions are ESR silent even at room temperature,<sup>10</sup> although the material is paramagnetic at temperatures higher than ca. 10 K. The

\* To whom scientific correspondence should be addressed. E-mail: okazaki@nirin.go.jp. Fax: 81-52-911-3351.

- (1) Yamanaka, S.; Sako, T.; Hattori, M. *Chem. Lett.* **1989**, 1869.
- (2) Fujita, W.; Awaga, K. *Inorg. Chem.* **1996**, *35*, 1915.
- (3) Fujita, W.; Awaga, K.; Yokoyama, T. *Inorg. Chem.* **1997**, *36*, 196.
- (4) Mori, W. Thesis, Osaka University, 1985, and private communication.
- (5) Oswald, H. R.; Feitknecht, W. *Helv. Chim. Acta* **1964**, *47*, 272.
- (6) Wells, A. F. *Structural Inorganic Chemistry*, 3rd ed.; Oxford: London, 1962.
- (7) Hoffmann, H.; Ulbricht, W. *Recent Res. Dev. Phys. Chem.* **1998**, *2*, 113.

- (8) Huo, Q.; Margolese, D. I.; Ciesla, U.; Feng, P.; Gier, T. E.; Sieger, P.; Leon, R.; Petroff, P. M.; Schuth, F.; Stucky, G. D. *Nature* **1994**, *368*, 317.
- (9) Beck, J. S.; Vartuli, J. C.; Roth, W. J.; Leonowicz, M. E.; Kresge, C. T.; Schmitt, K. D.; Chu, C. T.-W.; Olson, D. H.; Sheppard, E. W.; McCullen, S. B.; Higgins, J. B.; Schlenker, J. L. *J. Am. Chem. Soc.* **1992**, *114*, 10834.

molecular structure and magnetic properties of the complex will be discussed in detail.

### Experimental Section

Sodium dodecyl sulfate (SDS) of extra-pure grade from Nacalai Tesque (Kyoto, Japan) and 2,2,6,6-tetramethylpiperidine-*N*-oxyl (TEMPO) purchased from Sigma were used as received. Cupric chloride and cupric sulfate of guaranteed grade from Wako Pure Chemicals (Osaka, Japan) were also used as received. Elemental analysis for CHN was carried out with a CHN-corder (Yanako MT-3), and that for Cu was carried out by the ICP method using a Japan Jarrell Ash ICAP-1000S. Magnetic susceptibility measurements were made with a SQUID magnetometer (Quantum Design MPMS2) at 0.1 and 1.0 T. XRD analysis was made with a Rigaku RAD-II-B diffractometer. Surface area of the sample powder was measured by using an apparatus for the one-point BET method (FlowSorb II 2300, MicroMetrics). The ESR spectrum was observed with a Varian E-12 or a JEOL JES-RE1XM spectrometer at an ambient temperature (air conditioned) or at 77 K. High-resolution solid-state NMR was observed at room temperature by using a Bruker MSL-200 spectrometer with a magic angle spinning probe. The spinning frequency was about 2800 Hz. Spin lattice relaxation time for the carbon nucleus was determined by using Torchia's pulse sequence,<sup>11</sup> whereas that for alkyl proton was determined by the saturation recovery method. In the latter experiment proton magnetization was monitored through the carbon signal induced by cross polarization.<sup>12</sup>

### Results

Cupric chloride ( $\text{CuCl}_2 \cdot 2\text{H}_2\text{O}$ ; 3 mmol) was dissolved in a 0.2 M SDS solution (50 mL) with/without a spin probe (TEMPO, 1.0 mM), and the reaction was started by bringing the pH to ca. 6.8 with 1.0 M sodium hydroxide or 2.5% aqueous ammonia solution. The suspension was gently agitated with a magnetic stirrer during the synthesis. The reaction was stopped after the suspension showed an opalescence-like optical reflection, by which the growth of the particle is identified. The suspension was centrifuged to separate the precipitate and washed at least three times with distilled water. The scale-like precipitate was then dried in an evacuated desiccator. All these operations for synthesis and purification were made at ambient temperature. When NaOH is used for neutralization, the reaction temperature should be a little below 300 K; otherwise, the precipitate turns black to form cupric oxide.

The CHN contents were 32.53%, 6.34%, and 0.0%, respectively, which are very close to the theoretical values of 32.5%, 6.36%, and 0.0% for  $\text{Cu}_2(\text{OH})_3\text{DS}$ . The copper content measured by the ICP-ES method was 26.3%, which is also close to the theoretical value of 28.66%. The ash left after the CHN analysis is cupric oxide, from the weight of which the content of copper was determined to be 28.3%. Many basic copper salts  $\text{Cu}_2(\text{OH})_3\text{X}$  are known, e.g., basic copper chloride, bromide, and acetate, etc., while that of dodecyl sulfate anion has not been reported yet. From the XRD analysis, it has been determined that the bluish-green complex has a lamellar structure with a spacing of 2.64 nm. As mentioned above, only the botallackite structure is suitable for accommodating a long alkyl chain as the spacer between the two  $\text{Cu}_2(\text{OH})_3$  layers. In addition, the alkyl groups should be arranged as a monolayer phase, since the dodecyl sulfate ion in the all-trans conformation is as long as 2.1 nm.

Figure 2 shows the high-resolution solid-state  $^{13}\text{C}$  NMR spectra of  $\text{Cu}_2(\text{OH})_3\text{DS}$  (a) and SDS (b). Since the total features

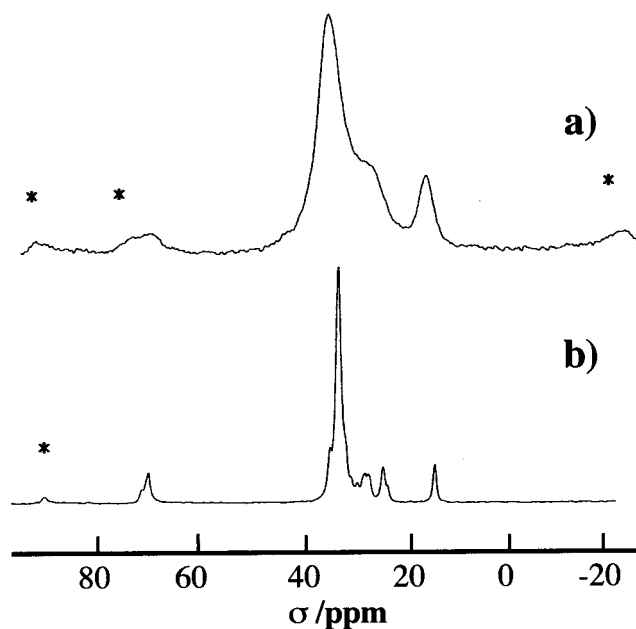


**Figure 2.** High-resolution solid-state  $^{13}\text{C}$  CPMAS NMR spectra for (a)  $\text{Cu}_2(\text{OH})_3\text{DS}$  and (b) SDS crystal. The number of transients for the accumulation were 264 and 64, respectively. The recycle delay was 5 s, and the contact time was 3 ms. Asterisks indicate the rotational sidebands (2.8 kHz).

(except the line width) of these two spectra are almost equal to each other, the dodecyl sulfate ion is undoubtedly kept chemically intact in the complex. The sharp peak (ca. 40 Hz of full width at half-height; fwhh) for the methyl carbon (C1) and that of most methylene carbons (C3–C11) of the SDS crystal appear at 14.7 and 33.0 ppm, respectively, from TMS (tetramethylsilane). These chemical shift values are typical of the alkanes and the alkyl groups. On the other hand, the corresponding signals of the copper complex are shifted toward the lower field by about 1.5 ppm and are broadened considerably to about 180 and 260 Hz (fwhh), respectively. These observed differences in both chemical shifts and line broadenings must be due to the paramagnetism of the cupric ions. In the case of the copper(II) salt of palmitic acid,  $\text{Cu}(\text{C}_{14}\text{H}_{29}\text{CO}_2)_2$ , whose structure is a simple bilayer one, the methyl peak of the  $^{13}\text{C}$  CPMAS NMR spectrum is much sharper (fwhh  $\approx$  90 Hz) compared with the above result, although that for the methylene carbon next to the carboxyl group is broadened to ca. 500 Hz.<sup>13</sup> The extended broadening of the methyl group in  $\text{Cu}_2(\text{OH})_3\text{DS}$  indicates that the methyl group is in close proximity to the cupric layer. This is one piece of evidence for the monolayer structure of the present complex.

Spin lattice relaxation measurements were made to obtain further information about the structure and the dynamics of the present system. The values of  $T_1$  of carbon ( $T_{1\text{C}}$ ) for the main  $\text{CH}_2$  chain were 2.5 and 1.5 s for the SDS crystal and the  $\text{Cu}_2(\text{OH})_3\text{DS}$  crystal, respectively. This small difference indicates that most of the methylene carbons in  $\text{Cu}_2(\text{OH})_3\text{DS}$  are not very close to the cupric ions. In the case of  $T_{1\text{H}}$  ( $T_1$  of proton), on the other hand, a large difference was found: the values are 1.2 s and 19 ms, respectively. This short  $T_{1\text{H}}$  and a relatively long  $T_{1\text{C}}$  for the alkyl group in the latter system can

(10) Mehran, F.; Barnes, S. E.; Chandrashekar, G. V.; McGuire, T. R.; Shafer, M. W. *Solid State Commun.* **1988**, *67*, 1187.

(11) Torchia, D. *J. Magn. Reson.* **1978**, *30*, 613.

(12) Okazaki, M.; Toriyama, K. *J. Phys. Chem.* **1989**, *93*, 2883.

(13) Toriyama, K.; Okazaki, M. Unpublished work. In the case of  $\text{Cu}(\text{II})$  palmitate two atoms (O and C) exist between the nearest alkyl carbon and the cupric ion, instead three atoms (S and two O) for  $\text{Cu}_2(\text{OH})_3\text{DS}$ . Thus it is natural that the larger line width of 500 Hz is observed for the nearest carbon in the former system than the corresponding one (260 Hz) in the latter.

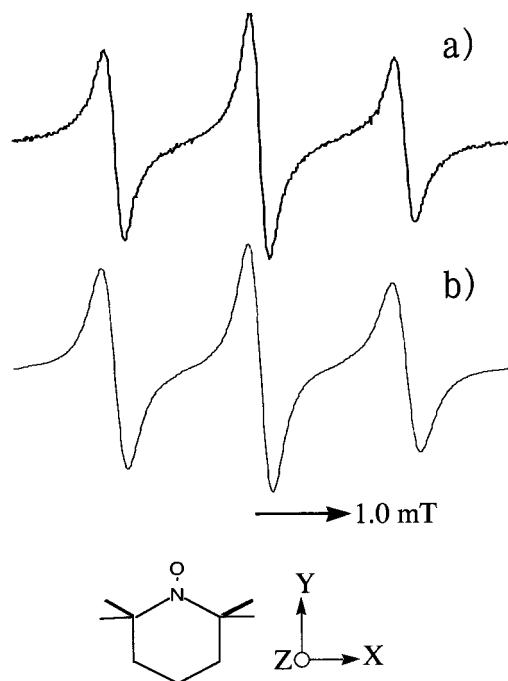


**Figure 3.** ESR spectrum of TEMPO radical introduced in the system to probe the alkyl layer (a) and its simulation by assuming that the TEMPO molecule rotates preferentially along its  $x$ -axis (b). The molecular structure and the rotational axes of TEMPO molecule are also shown.

be explained by the model that the excess Zeeman energy on the protons (supplied by the rf field) is not dissipated on the spot but is transferred along the alkyl chain to the OH protons, where the energy is discarded to the lattice. This is possible since the OH proton has a very short  $T_{1H}$  due to the interaction with the paramagnetic cupric ions, and the spin exchange within the alkyl protons is very rapid ( $\approx 10^4 \text{ s}^{-1}$ ).<sup>14</sup> Therefore spin exchange between the OH proton and the alkyl proton at the end is the rate-determining step for the  $T_{1H}$  process. This last step must be considerably slow because (1) the distance between the two protons is as far as 0.6 nm,<sup>15</sup> and the overlap between the two NMR lines, which is a necessary condition for a rapid spin exchange, may be small due to the NMR-line broadening for the OH proton caused by the paramagnetic cupric ion; and (2) the excess Zeeman energy on all the methyl and methylene protons (25 H) should be transferred and discarded on one or two OH protons. Thus the short  $T_{1H}$  of 19 ms is easily understood if the methyl protons are also in the proximity of the cupric layer. Although further quantitative analysis is difficult, this model for the proton spin relaxation is in agreement with the structure of Figure 1 and also with the observed  $T_1$ 's. Since the Zeeman splitting of the carbon nucleus is about  $1/4$  of that of proton, the alkyl carbons cannot make rapid spin exchange with the OH protons and thus the carbon relaxation is not accelerated by this mechanism.

The ESR spectrum of the TEMPO molecule doped in the alkyl layer is shown in Figure 3, which consists of three hyperfine components due to the nitrogen nucleus. This well-resolved three-line spectrum indicates that the spin probe is not

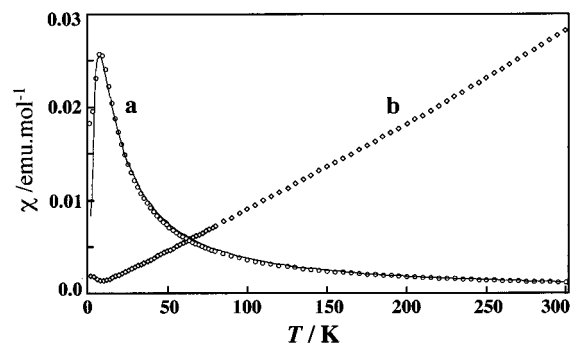


**Figure 4.** Magnetic susceptibility of  $\text{Cu}_2(\text{OH})_3\text{DS}$  at 1.0 T (a) and the inverted value (b). The simulation curve is a calculated one for a four-center model (see text).

trapped in a rigid medium but trapped in a more soft medium. The relative intensities of the hyperfine lines are typical for the TEMPO radical rotating preferentially around its  $x$ -axis (defined below the spectra). In fact, through simulation of the spectrum (spectrum b),<sup>16</sup> the rotational diffusion rate along the  $x$ -axis was determined to be 20 times as fast as that along the other two axes. Here it should be noted that the shape of the TEMPO radical is approximately prolate with the longer axis corresponding to the  $x$ -axis. These observations can only be explained by the model that the alkyl groups of the DS anions are aligned parallel to each other as in the lipid phase of a biological membrane and the spin probe is accommodated in this phase with the long axis along the dodecyl chains.<sup>17</sup> In fact the hyperfine splitting of 1.51 mT (Figure 3) indicates that the TEMPO molecule is dissolved in a hydrophobic environment.<sup>18</sup>

Figure 4 shows the magnetic susceptibility (circles) and its inverse value (squares) of the present system measured at 1.0 T as a function of temperature. Since the susceptibility decreases toward zero with lowering the temperature below 8 K, an antiferromagnetic interaction of ca. 8 K should exist in this system. The plot of  $1/\chi$  against  $T$  becomes almost linear in the temperature range higher than 200 K, and extrapolation of this region to the  $x$ -axis gives a Weiss constant of around 10 K. Therefore, a ferromagnetic interaction also exists in the system and is stronger than the antiferromagnetic one. The curve drawn with a solid line is a simulation for the susceptibility and will be mentioned later. The measurement was also made in the field of 0.1 T, where the susceptibility became a little smaller at temperatures below 15 K and the peak found at around 8 K in 1.0 T shifted to ca. 11 K. The lower temperature for the peak susceptibility at the higher magnetic field is easily explained by spin-canting to the magnetic field for the two groups of spins on the antiferromagnetic sublattices.<sup>2</sup> This mechanism is also confirmed by the fact that the observed  $\chi$  at about 2 K (the lowest temperature) remains much higher than the calculated value.

Figure 5 shows the ESR spectra of the present system under various conditions. Spectra a and b were those observed at an ambient temperature before and after evacuation for about 1 h, respectively. Spectrum c is that observed at 77 K, which was simulated as spectrum d. In spectrum a, we can see only a singlet at  $g \approx 2.20$  in the range  $0 \leq B_0 \leq 500 \text{ mT}$ . In spectrum b the main signal changes into one which is typical for randomly oriented cupric ions having an axially symmetric  $g$  tensor. Only

(14) The main mechanism for proton spin exchange is the dipole-dipole interaction. Thus, the spin exchange rate between the two protons separated by 0.15 nm is calculated as about 20 kHz.

(15) If we postulate standard bond lengths and their angles, we obtain 0.60 nm for the distance between Cu and the nearest alkyl carbon. So, the distance between the first alkyl proton and the OH proton may be almost equal to this value.

(16) Okazaki, M.; Kuwata, K. *J. Phys. Chem.* **1984**, *88*, 4181.

(17) Seelig, L. In *Spin Labeling*; Berliner, L. J., Ed.; Academic Press: New York, 1976; Chapter 10.

(18) Kawamura, T.; Matsunami, S.; Yonezawa, T.; Fukui, K. *Bull. Chem. Soc. Jpn.* **1965**, *38*, 1935.



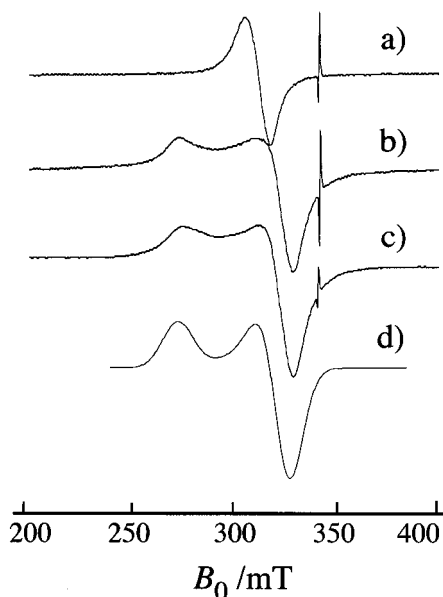


**Figure 5.** ESR spectra of  $\text{Cu}_2(\text{OH})_3\text{DS}$  before (a) and after (b) evacuation for about 1 h at ambient temperature, chilled at 77 K (c), and a simulation spectrum (d). The sharp signal at around 337 mT is due to DPPH marker (phase is reversed). Simulation was made assuming a  $\mathbf{g}$  tensor whose principal values are (2.10, 2.10, 2.49) and the line width of 15 mT.

slight changes were observed in spectrum c upon lowering of the temperature to 77 K. The parallel and perpendicular components of the  $\mathbf{g}$  tensor were determined as 2.49 and 2.10, respectively, by simulation d. Since the  $g$  factor of the singlet peak in spectrum a is nearly equal to the average of the  $g$  components for spectra b and c, spectrum a should be due to the same radical center. We consider that, in the system for spectrum a, a dynamic process averaged the  $\mathbf{g}$  tensor imperfectly, since the line shape remains asymmetric. It should be noted that the hyperfine structure is missing in all the spectra, that is usually observed in the parallel component of the spectrum for Cu(II) in a tetragonal field. Since  $g$  anisotropy is observed clearly, the missing hyperfine structure indicates that the radical center migrates among many cupric ions which have the same principal axes for the  $\mathbf{g}$  tensor. Another important fact is that the ESR response is much lower than that expected from the electron spin density. Thus most of the cupric ions are ESR silent. A very broad but weak signal was observed throughout the range  $0 \leq B_0 \leq 500$  mT for the degassed sample, but the spectral feature changed from sample to sample. Finally we have to mention that the sample had been treated repeatedly with water in the preparation to remove ionic impurities, and also that the experiments were repeated many times, confirming the same results. Therefore the signal is not due to an impurity, such as  $\text{Cu}^{2+}$  as a surface contamination.

## Discussion

**(1) Monolayer vs Bilayer.** In the preceding section we proposed that the newly prepared complex of  $\text{Cu}_2(\text{OH})_3\text{DS}$  has a monolayer structure of a botallackite type based on the observations of XRD,  $^{13}\text{C}$  CPMAS NMR, and spin probe ESR. Therefore the unit cell dimensions for “b”- and “c”-axes may be almost the same as those of botallackite:  $b = 0.6126$  nm,  $c = 0.5632$  nm, and that for “a” must be elongated from 0.5715 for botallackite (anion =  $\text{Cl}^-$ ) to 2.64 nm, as determined, to accommodate  $\text{C}_{12}\text{H}_{25}\text{SO}_4^-$  between the layers. The monolayer structure has been proposed by the fact that the spacing of 2.64

nm is not sufficient to form a bilayer for DS anions, since the length of DS anion with the all-trans conformation is as long as 2.1 nm including the van der Waals radius of the terminal methyl group. By subtracting the length of DS anion only 0.5 nm is left for the thickness of the cupric layer.<sup>1–3</sup> A modified botallackite structure has also been proposed for basic copper acetate  $\text{Cu}_2(\text{OH})_3\text{CH}_3\text{COO}$ , which is obtained by replacing  $\text{Cl}^-$  of botallackite with acetate ion. The methyl groups of the two adjacent layers are extruded to fill the common space as if they interlock the two  $\text{Cu}_2(\text{OH})_3$  networks.<sup>1</sup> As a similar example Kopka et al. showed that an alkyl sulfate complex of Zn–Cr hydroxide ( $\text{Zn}^{\text{II}}\text{Cr}^{\text{III}}(\text{OH})_6\text{DS}$ ) forms a monolayer alkyl phase, and a bilayer structure is formed only if dodecyl alcohol is added to the system.<sup>19</sup> In the botallackite-type structure for the present complex, the dodecyl group of one DS anion in the unit cell is extruded to the  $+a$  direction and the other DS anion to the  $-a$  direction from the  $bc$  plane of the crystal (Figure 1); thus the area on the plane allocated for one DS anion stretched to one direction is ca.  $0.345$  nm<sup>2</sup> ( $bc$ ), which is a little larger than 2.6 times the sectional area of the alkyl chain (about  $0.132$  nm<sup>2</sup>). It is well-known that the structure of a molecular assembly made of a surfactant is determined by the ratio between the sectional area of the head polar group ( $S$ ) and that of the alkyl chain ( $S_L$ ):  $P = S/S_L$ , which is called the shape factor.<sup>20</sup> It has been shown that  $P$  must be in the range  $1 \leq P \leq 2$  for the bilayer structure.<sup>7</sup> In the present case the area allocated for each DS anion ( $0.345$  nm<sup>2</sup>) should be considered as  $S$ , and thus the shape factor  $P \approx 2.6$ , which is not in the range for the bilayer structure. Above all, a monolayer arrangement of the alkyl chain is quite reasonable for the present complex also from the surface-chemical point of view. Although Fujita et al.<sup>3</sup> suggested that the chloride ion of botallackite is replaced with a long alkyl carboxylate anion ( $\text{C}_n\text{H}_{2n+1}\text{COO}^-$ ;  $n = 7–9$ ) to form a botallackite-like bilayer structure, we consider that it is not easy for these modified botallackite systems to form bilayer structures.

**(2) Magnetic Susceptibility.** The exchange interaction between a pair of adjacent electron spins in the present system is either ferromagnetic or antiferromagnetic. As indicated above, the magnitude of the former is a little larger than that of the latter. As shown in Figure 4, the antiferromagnetic interaction becomes apparent at temperatures lower than 8 K, so the approximate magnitude is easily estimated as being ca. 8 K. Although we have the Weiss constant of 10 K obtained from the plot of  $1/\chi$  vs. temperature, it does not coincide with the magnitude of the ferromagnetic interaction, because an antiferromagnetic interaction also exists in the system. So, we have tried a simulation with a model as shown in Figure 6, where two pairs of spins interact ferromagnetically within each pair and the two adjacent spins belonging to the different pairs interact antiferromagnetically. According to the model, the Hamiltonian  $\mathbf{H}$  of the system can be written as

$$\mathbf{H} = -2J(\mathbf{S}_1\mathbf{S}_2 + \mathbf{S}_3\mathbf{S}_4) - 2J^*(\mathbf{S}_2\mathbf{S}_3 + \mathbf{S}_4\mathbf{S}_1) + g\beta \sum_i \mathbf{B}\mathbf{S}_{i_z} \quad (1)$$

where  $J$  and  $J^*$  are the exchange interactions,  $\mathbf{S}_i$  is the spin operator for the  $i$ th ion,  $\mathbf{B}$  is the magnetic field, and  $g$  and  $\beta$  are the  $g$  value and the Bohr magneton, respectively. Upon diagonalizing the Hamiltonian we obtain the energy level shown on the right of Figure 6, where  $J$  and  $J^*$  are assumed as being

(19) Kopka, H.; Beneke, K.; Lagaly, G. *J. Colloid Interface Sci.* **1988**, *123*, 427.

(20) Israelachvili, J. N.; Mitchell, D. J.; Ninham, B. W. *J. Chem. Soc., Faraday Trans.* **1976**, *72*, 1525.

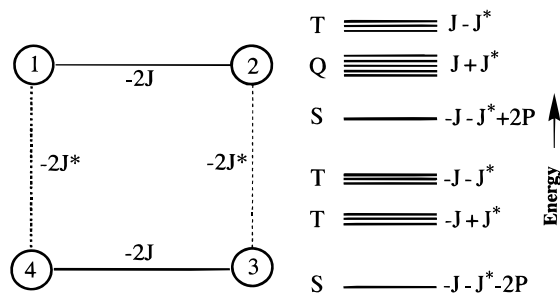


**Figure 6.** Four-center model for spin clustering in the present system. The exchange interaction  $-2J$  works between  $\text{Cu}(\text{II})$ 's (1,2) and (3,4) and that of  $-2J^*$  between (1,4) and (2,3). Exchange interaction for (1,3) and (2,4) is neglected. The energy levels of the system (S, singlet; T, triplet; and Q, quintet) is shown on the right, where  $P$  represents the square root of  $(J^2 + J^{*2} - JJ^*)$ .

positive and negative, respectively. It was also assumed that the absolute values of  $J$ ,  $J^*$ , and the difference  $(J - J^*)$  are much larger than the Zeeman term  $g\beta B$ . This means that we neglected state mixing between the different multiplets. The susceptibility  $\chi_M$  can be represented by the formula<sup>21</sup>

$$\chi_M = \frac{kTN_A}{4Z} \left( \frac{\delta Z}{\delta \mathbf{B}} \right) \frac{1}{\mathbf{B}} \quad (2)$$

where  $Z$  represents the distribution function of the system,  $N_A$  the Avogadro number,  $T$  the absolute temperature and  $k$  the Boltzmann constant. An explicit form of the equation for  $\chi_M$  was obtained by using the eigenvalues of eq 1 (shown at the right end of Figure 6):

$$\chi_M = \frac{g^2 \beta^2 N_A}{4kT} [10 \exp(-S) + 2\{\exp(\Delta) + \exp(-\Delta) + \exp(S)\}] / [5 \exp(-S) + 3\{\exp(\Delta) + \exp(-\Delta) + \exp(S)\} + \exp\{S + 2P\} + \exp\{S - 2P\}] \quad (3)$$

The symbols  $S$ ,  $\Delta$ , and  $P$  are defined below:

$$S = (J + J^*)/kT, \quad \Delta = (J - J^*)/kT, \\ P = (J^2 - JJ^* + J^{*2})^{1/2}/kT \quad (4)$$

The experimental data are reproduced fairly well as shown in Figure 4 with a solid line, by employing the parameters  $-7.0$  K for  $J^*$ ,  $45$  K for  $J$ , and  $2.20$  (observed by ESR) for the  $g$  value. The temperature independent paramagnetism can be neglected, since the contribution is very small for copper, though it becomes one of the main mechanisms for a rare earth element. In the simulation we had to assume that one-fourth of the cupric ions does not contribute to this magnetism. This may imply that we have to postulate one valence bond formation for every eight copper ions. Although we obtain the same simulation curve with a  $g$  value of  $1.905 (= 2.20\sqrt{3/4})$ , there is no physical basis for adopting this value. We could not find any further evidence for the cause of this interesting result. In the actual system many types of clusters may exist, thus the exchange interaction of  $45$  K is only a rough estimate. Important information extracted from the simulation is that (1) the ferromagnetic interaction is much stronger than the antiferromagnetic interaction of around  $10$  K and (2) electron spins make networks or clusters via these exchange interactions.

Since the interval between the two cupric layers is larger than  $2.6$  nm, an observable exchange interaction beyond this thick

layer cannot be expected. Thus, both the ferromagnetic and antiferromagnetic interactions must be intralayer ones. In the botallackite structure there are two kinds of cupric sites: in one case each cupric ion is bonded to four hydroxides and two DS anions [referred hereafter as  $\text{Cu}(4+2)$ ], while in the other case each cupric ion is bonded to four hydroxides in a usual manner, and another hydroxide with a longer bond length in addition to one DS anion [ $\text{Cu}(4+1+1)$ ].<sup>22</sup> The latter cupric ions make a coplanar  $\text{Cu}(\text{OH})_2$  array. On the other hand the former cupric ions change their principal axis ( $z$  direction of the tetragonal symmetry) alternately. Therefore there must be several different exchange interactions between the adjacent cupric ions: e.g., two are those between two ions in the same group, and another is between the two cupric ions belonging to the different groups. So, the model of Figure 6 is the simplest one for the present system. However, the details of these magnetic interactions are beyond the scope of the present study.

### (3) The Nature of the Defect Giving ESR Spectrum.

Generally speaking the ESR spectrum of an isolated cupric ion in a tetragonal field shows both  $g$  anisotropy and hyperfine structure. Therefore, the absence of hyperfine structure in spectra b and c of Figure 5 (showing only a  $g$  anisotropy which is typical for  $\text{Cu}(\text{II})$  in a tetragonal site) indicates that the ESR active site moves rapidly among the cupric ions having the same principal  $g$ -axes: i.e., this rapid two-dimensional movement averages the hyperfine structure leaving the  $g$  anisotropy invariant. This kind of dynamics is possible only on the chain of  $\text{Cu}(4+1+1)$ . As an extension of this model we consider that the radical center for the singlet peak ( $g = 2.20$ ) in spectrum a of Figure 5 may move over a wider range as to partly average not only the hyperfine structure but also the  $g$  anisotropy. If the electron spin moves over all the cupric ions, the  $g$  anisotropy is partly averaged and a single line may apparently be observed. This is because the averaging occurs among the three  $g$  tensors: two are for  $\text{Cu}^{2+}(4+2)$ , and the third is for  $\text{Cu}^{2+}(4+1+1)$ .<sup>23</sup> If we postulate the original  $g$  components to be  $(2.10, 2.10, 2.49)$  for  $x, y,$  and  $z$  components (principal axes are different among the three types of cupric ions), the weighed average values are  $(2.18, 2.17, 2.34)$ , whose principal axis almost coincides with the crystal axis.<sup>24</sup> Figure 7 shows the simulated spectrum (b) of this partially averaged powder ESR and the observed spectrum (a). Although the agreement is not perfect, the essential feature is reproduced satisfactorily in the simulated spectrum. Since this spectrum with the partially averaged  $g$  tensor appears for the system left in the moisturized atmosphere, the adsorbed water molecule may accelerate the mobility of the paramagnetic center (or defect) along the copper network. In addition to the doublet center, there should be high-spin paramagnetic centers which give a weak but very broad signal throughout the spectrum region. As for the origin of these paramagnetic centers

(22) The closed circle in Figure 1 at the center of the duplex line (four single bonds in total with OH groups) corresponds to  $\text{Cu}(4+1+1)$ . The rest of the closed circles correspond to  $\text{Cu}(4+2)$ .

(23) According to the crystal structure in ref 6, the axis of  $g$ -parallel for  $\text{Cu}(4+1+1)$  is invariant all over the crystallite but that of  $\text{Cu}(4+2)$  changes alternately.

(24) The three axes perpendicular to the  $\text{Cu}(\text{OH})_4$  planes were assumed to be the principal axes for the parallel components of the  $g$  tensors. By making use of the crystallographic data available from the Internet (JST crystal structure database) the directional cosines of the three principal axes  $(-0.8073, 0, 0.5902)$ ,  $(0.7215, 0.5972, 0.3504)$ , and  $(0.7215, -0.5972, 0.3504)$  were obtained, where the crystallographic axes  $a, b,$  and  $c'$  ( $La, b$ ) were taken for the coordinate. The two other axes for the perpendicular components of the  $g$  tensor can be chosen in the  $\text{Cu}(\text{OH})_4$  plane for each  $g$  tensor. Averaging of the four tensors, two of which are for  $\text{Cu}(4+1+1)$  and thus identical, and diagonalization were made in the usual manner.

(21) Ballhausen, C. J. *Introduction to Ligand Field Theory*; McGraw-Hill: New York, 1962; Chapter 6.

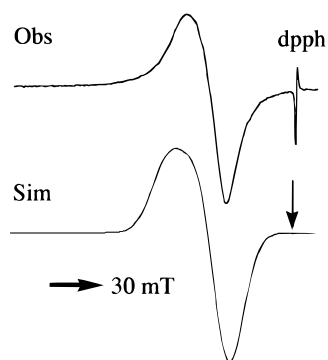


**Figure 7.** ESR spectrum of Cu(II) for the sample exposed with moisture (a) and its simulation (b). The simulation spectrum is that for randomly oriented cupric ions with the  $g$  tensor averaged over the three kinds of Cu(II) ions in the complex. Two of these belong to Cu(4+2), and the rest belongs to Cu(4+1+1), the latter of which was weighted twice in the averaging.

with higher spin states, we are considering transient spin clusters. Since a satisfactory simulation of the magnetic susceptibility (Figure 4) could be made with a spin cluster model of Figure 6, we consider that this kind of spin cluster is trapped temporally in a site for a short time ( $\geq$ nanoseconds). If some kind of defects, such as incompleteness in the ligand structure, exist in the atomic arrangement, a spin or cluster of spins may be stabilized there for a short time. When the lifetime is elongated to, say, several nanoseconds, their ESR spectra become observable.

**(4) Disappearance of the ESR Spectrum.** It is well-known that an ESR spectrum is observed for a paramagnetic species (whose orbital angular momentum is well quenched) such as cupric ion at a high temperature (298 K), even though it changes into a ferromagnet or an antiferromagnet at a low temperature. When the concentration of the paramagnetic ion is large, the ESR spectrum of this ion may be broadened by a spin exchange

interaction which partially averages the hyperfine structure. However, the total spectrum width does not exceed the range of the original hyperfine structure. With a further increase in concentration, spin exchange occurs faster, and the broadened structure is sharpened into a single line, as is the case for solid DPPH. For another example, a strong ESR spectrum without the hyperfine structure is observed for  $\text{CuCl}_2 \cdot 2\text{H}_2\text{O}$ , which has a strong antiferromagnetic interaction of ca.  $J = -78$  K. On the other hand, ESR response sometimes disappears in other cupric salts.<sup>10</sup> To the best of our knowledge the cause of ESR-signal disappearance has not been explained with an understandable mechanism. Mehran et al.<sup>10</sup> suggested that the disappearance of ESR signals for cupric oxide may have some relation with the “resonance valence bond” formation.<sup>25,26</sup> However, the valence bond formation throughout the crystal should decrease the magnetic susceptibility dramatically.

The model in Figure 6 demonstrates the interaction of four spins in which we find a quintet state and three triplet states as well as two singlet states. The transition of the system among these states generates a large fluctuating magnetic field, which makes ESR observation of the surrounding spins and spin clusters difficult. The size of the clusters is not limited to four spins, but is distributed from a few up to infinite. Therefore the ESR response can be observed only from a special position where the spin states are stabilized by some reasons.

**Acknowledgment.** We thank Prof. W. Mori of Kanagawa University for the magnetic susceptibility measurement and valuable discussions. Many thanks should go to several researchers of our institute, especially Dr. A. Tsuge, and Dr. H. Morikawa for chemical analysis, and Dr. S. Velu for improving the English.

IC000088H

(25) Anderson, P. W. *Science* **1987**, 235, 1196.

(26) Kivelson, S. A.; Rokhsar, D. S.; Sethna, J. P. *Phys. Rev.* **1987**, 35, 8865.